Helicobacter

Helicobacter ISSN 1523-5378
doi: 10.1111/hel.12321

Elucidation of the Metabolic Network of *Helicobacter pylori* J99 and Malaysian Clinical Strains by Phenotype Microarray

Woon Ching Lee,* Khean Lee Goh,† Mun Fai Loke* and Jamuna Vadivelu*

*Faculty of Medicine, Department of Medical Microbiology, University of Malaya, Kuala Lumpur, Malaysia, †Faculty of Medicine, Department of Medicine, University of Malaya, Kuala Lumpur, Malaysia

Keywords
Metabolism, phenotype microarray, carbon sources, amino acids.

Reprint requests to: Jamuna Vadivelu, Department of Medical Microbiology, Faculty of Medicine, University of Malaya, Jalan Universiti, 50603 Kuala Lumpur, Malaysia.
E-mail: jamuna@ummc.edu.my

Abstract

Background: *Helicobacter pylori* colonizes almost half of the human population worldwide. *H. pylori* strains are genetically diverse, and the specific genotypes are associated with various clinical manifestations including gastric adenocarcinoma, peptic ulcer disease (PUD), and nonulcer dyspepsia (NUD). However, our current knowledge of the *H. pylori* metabolism is limited. To understand the metabolic differences among *H. pylori* strains, we investigated four Malaysian *H. pylori* clinical strains, which had been previously sequenced, and a standard strain, *H. pylori* J99, at the phenotypic level.

Materials and Methods: The phenotypes of the *H. pylori* strains were profiled using the Biolog Phenotype Microarray system to corroborate genomic data. We initiated the analyses by predicting carbon and nitrogen metabolic pathways from the *H. pylori* genomic data from the KEGG database. Biolog PM aided the validation of the prediction and provided a more intensive analysis of the *H. pylori* phenomes.

Results: We have identified a core set of metabolic nutrient sources that was utilized by all strains tested and another set that was differentially utilized by only the local strains. Pentose sugars are the preferred carbon nutrients utilized by *H. pylori*. The amino acids L-aspartic acid, D-alanine, and L-asparagine serve as both carbon and nitrogen sources in the metabolism of the bacterium.

Conclusion: The phenotypic profile based on this study provides a better understanding on the survival of *H. pylori* in its natural host. Our data serve as a foundation for future challenges in correlating interstrain metabolic differences in *H. pylori*.

The microaerophilic bacterium *Helicobacter pylori* is a slow-growing bacterial pathogen present in almost half of the world population that establishes lifelong infections in humans. This bacterium lives within and beneath the mucus layer that covers the gastric mucosa. The most notable enzyme produced by this bacterium is the potent urease that enables it to survive acidic conditions by hydrolyzing urea to carbon dioxide and ammonia. This local neutralization of gastric acid helps *H. pylori* to successfully colonize the gastric epithelium [1]. The presence of *H. pylori* in the gastric mucosa is strongly associated with peptic ulcer disease (PUD) and nonulcer dyspepsia (NUD) and is implicated in more severe gastric diseases, including gastric adenocarcinoma. The nature and severity of the disease may be highly variable depending on the both host and bacterial characteristics, which include their genotypes [2]. The genetic variation among the strains has been suggested to be responsible for the disparities of symptoms in *H. pylori*-infected patients [3]. The evolution of specific genes and proteins in this pathogen is of paramount importance in this field as it strives to understand the role of specific genes in its virulence.

At the genomic level, *H. pylori* is well characterized as there are many strains that have had their whole genome sequenced. Bacterial genomics, the identification and annotation of the entire coding potential of a bacterium, allows a more complete physiological

integration of phenotypic characteristics of an organism based on functional identification of genes and reconstruction of the metabolic network [4,5]. Metabolism involves the production of mass, energy, and redox requirements for all cellular functions, and thus provides the driving force for cellular activity. However, these genomic analyses provide only an in silico estimate of overall metabolism of *H. pylori*. The ability of human pathogens to metabolize various nutrients is essential for the invasion, growth, survival, and colonization in their hosts. To successfully colonize and persist in the various niches within the host during the course of infection, pathogenic bacteria need to adjust and adapt their metabolic activity according to the local nutrient availability. However, as compared to the growing knowledge of molecular bacterial virulence and pathogenesis, research on *H. pylori* metabolism and persistence in the human host has very little progress over the years. Having evolved and persisted in the human gastric niche for many years, the adaptation of *H. pylori* in its human host should be reflected in a unique complement of physiological capabilities. Phenotype MicroArray™ (PM) technology by Biolog is able to reveal many aspects of the bacterial cellular phenotype. The test uses tetrazolium redox chemistry which produces a color change in response to metabolically active bacterial cell respiration. This technology has been used to be able to explore and identify the unique metabolic traits of different bacterial strains [6].

The clinical strains used in this study were isolated from gastroduodenal ulcer patients who went for gastroscopy at University of Malaya Medical Centre (UMMC), Kuala Lumpur, Malaysia. *H. pylori* strains UM032 and UM066 were isolated from PUD patients, while UM037 and UM276 were from NUD patients. The *H. pylori* standard strain, J99, was isolated from a duodenal ulcer patient [7]. To reveal a more representative metabolic profile of the *H. pylori* strains, we investigated these four clinical isolates that were genomically sequenced and a standard strain, *H. pylori* J99, at the phenotypic level using the OmniLog PM system to corroborate genomic data. We used Biolog plates PM1 to PM4, giving 190 carbon sources, 95 nitrogen sources, 59 phosphorous sources, and 35 sulfur sources, and the PM9 and PM10 plates, giving 192 tests of environmental conditions such as pH and salt concentrations, to assess whether they could be discriminated based on their respiration profiles, and at the same time, establish whether PM high-throughput would define potential differential markers for *H. pylori*. Integration of phenomics into genomic information will serve to deepen our knowledge of the metabolic diversity of this bacterium. A better understanding of the biochemistry of *H. pylori* is of fundamental interest to microbiology and could also help in developing new anti-*H. pylori* therapy.

Methods

Bacterial Cultivation

Four clinical isolates of *H. pylori* (UM032, UM037, UM066, and UM276) available in our culture library and the standard strain J99 (ATCC, Manassas, VA) were selected for the present work. After minimal passage, the isolates were stored in brain heart infusion (BHI) medium with 20% glycerol at −80 °C. All the *H. pylori* strains, including J99, were revived by inoculating them onto chocolate agar (supplemented with 7% lysed blood), which were then incubated for 3 days in humidified air with 10% CO_2 at 37 °C.

Characterization of Strains by Phenotype MicroArray

The PM assay was performed using the 96-well microplates PM1, PM2A, PM3B, PM4A, PM9, and PM10 (http://www.biolog.com/pdf/pm_lit/PM1-PM10.pdf) [8] to determine the metabolic profiles of *H. pylori*. All the materials, media, and reagents required for the PM system were purchased from Biolog (Hayward, CA). The experiment was conducted according to the procedures developed by the manufacturer with slight modifications to the bacterial cultivation. Briefly, *H. pylori* cells cultured on the heavily streaked chocolate agar, which had been passaged fewer than three times from the frozen stock, were harvested using sterile swab and transferred into inoculating fluid to achieve 16% transmittance (T). Cell suspensions at the final cell density of 52% T (72% T for PM9 and PM10) were supplemented with a final concentration of 0.05% BSA and 1.25 mmol/L $NaHCO_3$. An additional carbon source of glucose was added into the cell suspension for the plates PM3B, PM4A, PM9, and PM10 to the final concentration of 2.5 mmol/L. To these suspensions, the redox indicator tetrazolium (dye D) was added at a final concentration of 0.01%. One hundred microliter of the final cell suspensions was loaded into each well of the PM microplate. All the plates, together with a CO_2 Compact sachet (Oxoid, cat. no. CD0020C), were sealed in a gas-impermeable bag and incubated at 37 °C in an OmniLog incubator. The colorimetric readings were recorded for 60 hours, and the data were evaluated using OmniLog PM software. The assay was performed in duplicates.

 22: e12321, DOI: 10.1111/hel.12321

Data Analysis

During the colorimetric measurements, the well A01 (negative control) was monitored to ensure the absence of kinetic activities. At the end of the incubation period, the reduction in reporter dye was expressed as OmniLog units. To compare the utilization of different metabolic compounds, the raw data, including the parameters slope, maximum (Tmax), and minimum (Tmin) readings, were exported from the software. The opm package in R-project [1] was used to reconstruct the kinetic curves. The integrated surface area under the time course kinetic curves (AUC) that reflected the metabolic activity values was extracted from the software.

To assess the metabolic kinetic activities in each well, the slope was first used to determine positive growth under various PM conditions. The values of average AUC for all the negative wells were calculated to obtain the background value so that a threshold can be determined to offset the average area obtained in each well with positive growth for each strain in PM 1–4. For PM9 and 10, as there is no negative control well, the difference of the kinetic data (Tmax−Tmin) was obtained and expressed as relative OmniLog units.

Bioinformatics Analysis

The RAST web server [9] was used to automatically annotate the genome sequences. Annotated proteins sequences were used to map against KEGG pathway databases (KEGG (http://www.genome.jp/kegg) to determine metabolic pathways to which the proteins were assigned [10]. The respective orthologue tables, KEGG module, and KEGG compound were extracted to construct metabolic maps. Homology searches were performed using the BLASTN tools [11].

Validation of PM Data to Confirm Utilization of β-cyclodextrin as Carbon Substrate

After the completion of PM analysis, β-cyclodextrin was selected for further validation of the metabolic activity measured with Biolog PM technology. This cyclic oligosaccharide is commonly added in the liquid media to cultivate *H. pylori*. To confirm the PM analysis results, which showed that the compound was not metabolized by the strains, the utilization of β-cyclodextrin was subsequently investigated by performing independent studies in four types of media, without using the PM plates. All the five strains were inoculated into BHI, BHI supplemented with 1% of β-cyclodextrin, IF-0a inoculation fluid (Biolog) as well as IF-0a supplemented with 1% of β-cyclodextrin, respectively. The cells were incubated in inoculation flasks at 37 °C. A positive growth is determined in duplicate based on the OD600 reading of the culture in every 24 hour. Experiments were repeated at least twice.

Results

The four *H. pylori* strains used in this study were chosen because their genomes were previously sequenced [12,13] and the complete genome sequence of the reference strain J99 can be obtained in GenBank (accession number NC_000921.1). The kinetic curves of PM analysis are shown in Fig. S1, and the nutrient sources utilized by strains as indicated by PM data are summarized in Table S1 and Fig. 1.

Carbon Source Utilization (PM1 and PM2A)

Using Biolog PM1 and PM2, 190 different carbon sources were tested on the five strains of *H. pylori*. *H. pylori* J99 was able to metabolize 49 (25.8%) of the tested carbon sources, while the Malaysian clinical strains UM032, UM037, UM066, and UM276 metabolized 50 (26.3%), 38 (20.0%), 56 (29.5%), and 38 (20.0%) compounds, respectively. Only 25 compounds of the carbon sources tested were metabolized by all the five strains (Fig. 2). These include the amino acids (L-aspartic acid, D-alanine, D-serine, and L-asparagine), metabolic pathway intermediates (succinic acid and its derivative D-glucuronic acid, D,L-malic acid, D-fructose-6-phosphate, fumaric acid, bromosuccinic acid, L-malic acid, pyruvic acid, 5-keto-D-gluconic acid, succinamic acid, and dihydroxyacetone), and carbohydrates (L-arabinose, D-galactose, L-fucose, D-xylose, D-ribose and its

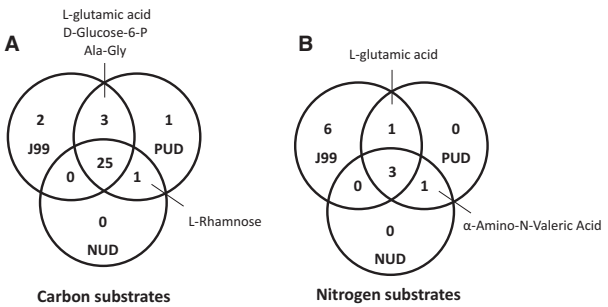

Figure 1 Venn diagrams showing (*A*) carbon substrates and (*B*) nitrogen substrates catabolized by *H. pylori* strains isolated from PUD and NUD patients. The capabilities of the strains in utilizing the substrates during metabolism may be responsible for the disease outcomes. Nevertheless, the sample size needs to be increase in order to confirm this notion.

derivative 2-deoxy-D-ribose, D-psicose, L-lyxose, glucuronamide, and D-arabinose). Only two carbon sources were metabolized by *H. pylori* J99, but not the Malaysian clinical strains, which are the dipeptide gly-glu and glycogen. In contrast, the sugar L-rhamnose was used by all the Malaysian clinical strains but not the *H. pylori* J99.

Nitrogen Source Utilization (PM3B)

There are only three compounds of the 95 nitrogen sources that serve as the core metabolic nutrient sources for *H. pylori*. Compounds used by all the strains during their respiration are the amino acids (L-asparagine, L-aspartic acid, and D-alanine) and are also the core carbon sources for all the strains tested for their metabolism. *H. pylori* J99 metabolized amino acids or their derivatives (L-arginine, L-proline, L-ornithine, N-phthaloyl-L-glutamic acid, gly-asn, and gly-glu) that the other strains did not utilize for respiration. In contrast, among the strains tested, only *H. pylori* J99 showed no respiration with α-amino-N-valeric acid.

Phosphorus and Sulfur Source Utilization (PM4A)

The *H. pylori* strains did not metabolize much of the phosphorus and sulfur sources for growth. There are no substances identified as core nutrients during the respiration of the strains in the plate PM4A. All the strains except *H. pylori* J99 utilized dithiophosphate (phosphorus source). *H. pylori* J99 did not appear to utilize phosphorus compounds, whereas *H. pylori* UM037 did not utilize sulfur compounds in their respiration process. The lack of phosphorus utilization may be explained by the presence of polyphosphate granules in the cell [14]. The granules serve as energy and phosphorus storage and participate in the regulation of various metabolic processes of *H. pylori*. Accumulation of polyphosphate granules is more prominent in the viable but nonculturable (VBNC) coccoid than in the spiral form [15] suggests that phosphorus compounds may not be essential to *H. pylori* for growth. This is not unexpected as polyphosphate kinase (PPK) in *H. pylori* is not required in the bacterial growth but is essential for colonization [16].

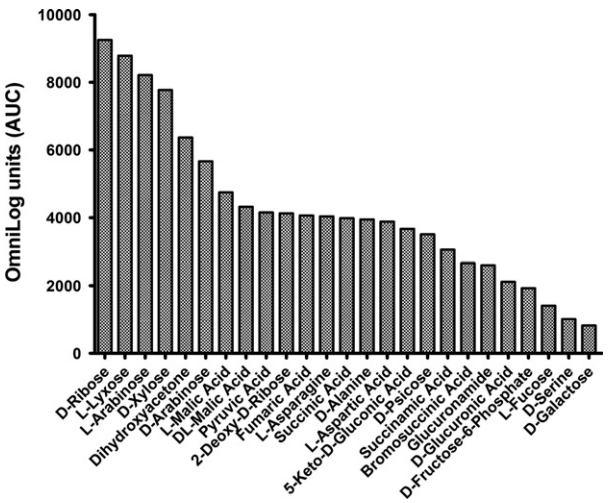

Figure 2 Carbon substrates that are commonly utilized by all the *H. pylori* strains. The average area under the curve, AUC, of the kinetic data for the five strains was obtained. Dye reductions were higher in the metabolism of pentoses, more specifically, the aldopentoses (ribose, lyxose, arabinose, and xylose). This suggests that these aldopentoses are the preferred energy sources used by the bacteria during their respiration.

Effects of Osmolytes and pH (PM9 and PM10)

The strain UM032 showed better osmolytes tolerance compared to the other strains tested. The survival of *H. pylori* strains in a range of sodium chloride (NaCl) concentration showed an interesting pattern (Fig. S4A). The strains survived best at 1% NaCl (2% for UM032), and their metabolism was lowest at 3–4% NaCl. The metabolism gradually increased from 5% NaCl and reached another lower peak at 7–8% NaCl.

In general, *H. pylori*, especially strain UM032, showed the ability to survive in a wide range of chemical compounds that could be present in human stomach, including urea and food additives or preservatives. It is however not surprising that *H. pylori* could survive in the presence of urea. Current observation (Fig. S4B) shows that the *H. pylori* strains other than UM032 had better respiration at the highest urea concentration (7%, PM9 well E07).

The bacterial metabolism is also affected by pH. As shown in Fig. S5, *H. pylori* strains have similar pattern of pH for metabolism and able to survive at pH >5, where the optimum range is at pH 5.5–7 (PM10, well A05-7). The drop in kinetic activity was observed at pH 8 and then increased slowly at pH >8.5. Besides, *H. pylori* performed better with various nitrogen compounds under pH 9.5 as compared to pH 4.5.

Role of β-Cyclodextrin

β-cyclodextrin was not involved in the metabolism of any tested strains. In the validation test (Fig. 3), the presence of β-cyclodextrin in BHI enhanced the growth of *H. pylori*. On the contrary, the minimal medium used for PM analysis did not support the growth of the bacteria even with the addition of β-cyclodextrin.

 22: e12321, DOI: 10.1111/hel.12321

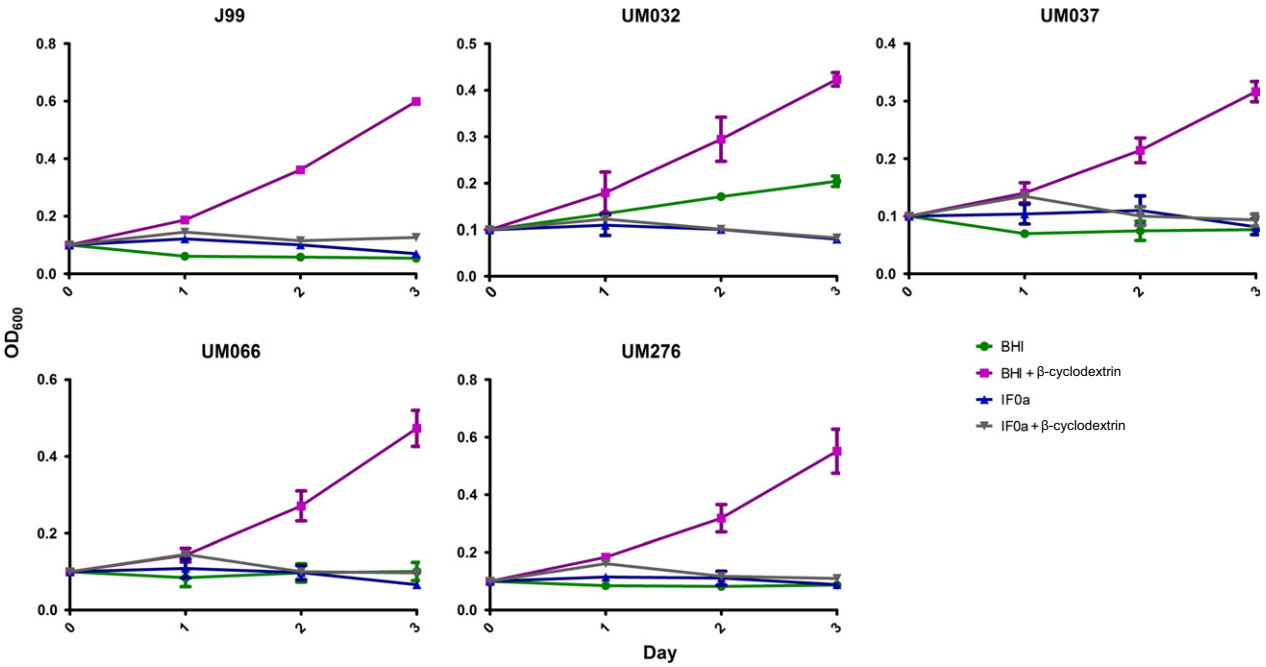

Figure 3 Effect of β-cyclodextrin in culturing media on the *H. pylori* growth. Error bars indicate mean ± SE of three independent experiments performed in duplicate. Growth was detected only in the BHI supplemented with 1% (w/v) β-cyclodextrin.

Particularly in UM032, this strain is able to show slight growth in BHI without β-cyclodextrin. Together with the absence of growth in the β-cyclodextrin-supplemented minimal medium IF0a, the results suggest that β-cyclodextrin does not act as a substrate for metabolism in *H. pylori*.

KEGG Observation

The RAST-annotated protein sequences from all the tested strains in this study were mapped against KEGG databases. The compounds predicted to be involved in metabolic pathways were compared to PM analysis. The proposed map for carbon metabolism was constructed and shown in Fig. 4, whereas the KEGG nitrogen metabolism map was shown in Fig. S2. The metabolism pathways are generally conserved among the strains, except for the enzymes that are listed in Table 1.

The orthologue of acetyl-coenzyme A synthetase that catalyzes the formation of acetate from acetyl-coenzyme A in the citric acid (TCA) cycle is not found in J99. Other enzyme orthologues (N-methylhydantoinase A, delta-1-pyrroline-5-carboxylate dehydrogenase, proline dehydrogenase (proline oxidase)/delta-1-pyrroline-5-carboxylate dehydrogenase) that were present in local *H. pylori* strains but not in J99 are involved in proline metabolism, which may explain the utilization of proline as both carbon and nitrogen sources in only the strain J99. Aspartate aminotransferase is used to catalyze the interconversion of L-aspartate and α-ketoglutarate to oxaloacetate and glutamate in TCA cycle. The orthologue of this enzyme is only found in J99 and UM037; however, the result from PM analysis does not agree with this observation as L-aspartate was utilized by all the tested strains as a carbon source.

Discussion

Because of its role as a causative agent of gastritis and stomach ulcers, *H. pylori* was one of the first bacterium to have its complete genome sequence published. As little is known about the metabolism of *H. pylori*, genome sequence data have been used to annotate the genes and predict the corresponding metabolic networks in *H. pylori*. In the present study, we integrate the phenotypic characteristics of the bacteria with the predicted pathways from KEGG. By applying data from the PM assays, a large number of additional nutrient sources utilized were revealed. The study also provides additional basic metabolic information for modeling and flux balance analysis.

Carbon as Metabolic Energy Source

Bacteria require a sufficient supply of carbon to feed their metabolic pathways. In their native environments,

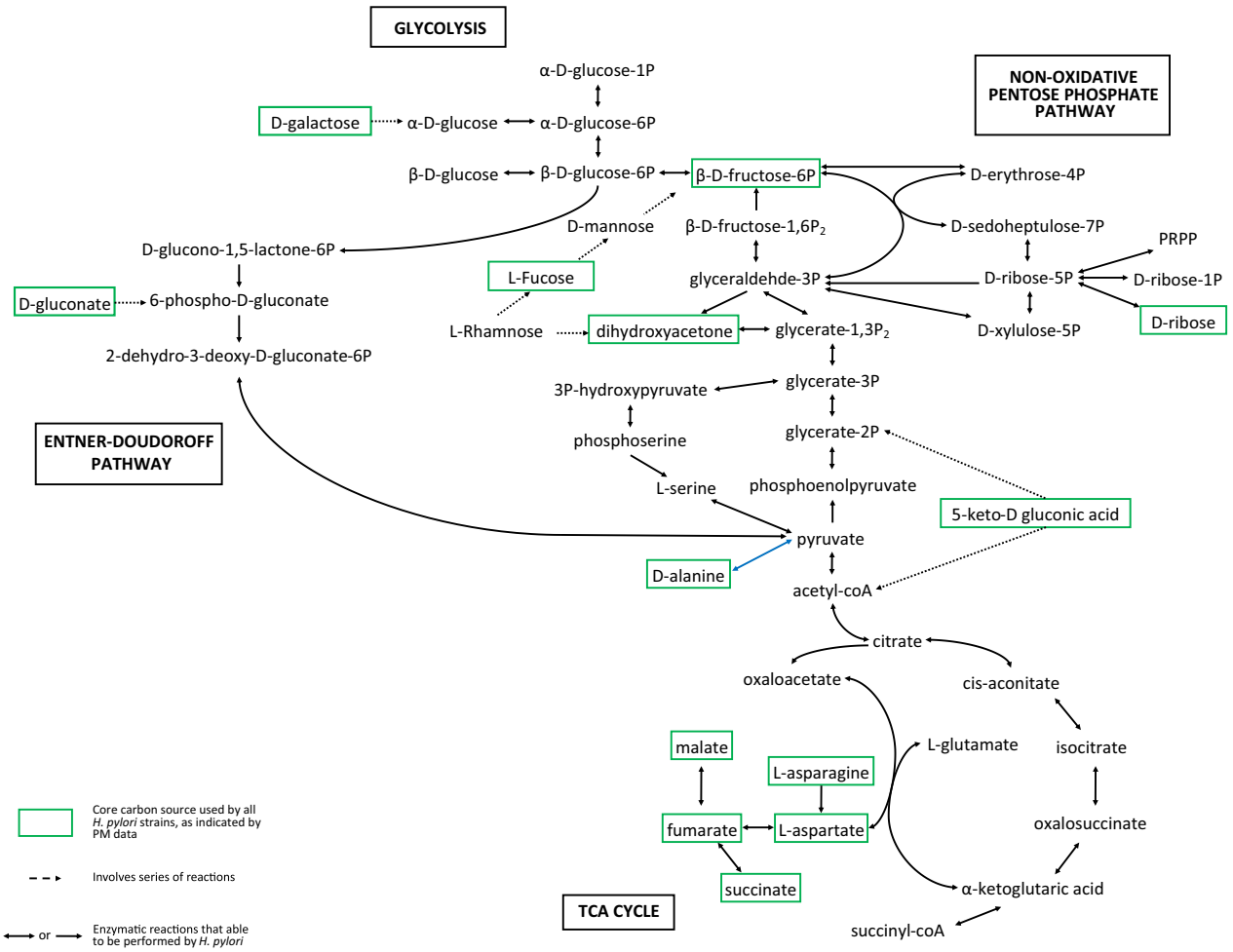

Figure 4 Proposed carbon metabolism in *H. pylori* based on PM analysis and KEGG pathway predictions. Blue arrow denotes the absence of enzyme orthologue in the reaction.

Table 1 Enzymes orthologues present in each *H. pylori* strains based on KEGG databases

Orthologues	KEGG enzyme entry	J99	UM032	UM037	UM066	UM276
Acetyl-coenzyme A synthetase	EC 6.2.1.1		•	•	•	•
N-methylhydantoinase A	EC 3.5.2.14		•	•	•	•
Delta-1-pyrroline-5-carboxylate dehydrogenase	EC 1.5.1.12		•	•	•	•
Proline dehydrogenase (Proline oxidase)/ Delta-1-pyrroline-5-carboxylate dehydrogenase	EC 1.5.99.8/EC 1.5.1.12		•	•	•	•
Aspartate aminotransferase	EC 2.6.1.1	•		•		

limited amounts of complex mixtures of carbon sources are often present at low concentrations. As a result microbial cells have developed multiple systems to utilize a wide array of different substrates as carbon sources. Since the discovery of *H. pylori*, complex sugars were predicted as not the major energy source while glucose appears to be the only carbohydrate utilized by this bacterium [17,18]. The application of PM analysis allowed us to identify additional carbon sources that could be metabolized by *H. pylori* strains.

Galactose (PM1, well A06) and fucose (PM1, well B04), which are monomers of sugars (hexose), were used by all the tested *H. pylori* strains. L-rhamnose (PM1, well C06), which was utilized by the local clinical strains only, can be converted into fucose or dihydroxyacetone in fructose and mannose metabolism.

These sugars will eventually enter the glycolytic pathway. *H. pylori* possesses genes for the glycolytic reactions required to convert glucose until D-fructose-6P. In this study, only *H. pylori* UM037 did not utilize α-D-glucose (PM1, well C09), whereas only J99, UM032, and UM066 utilized D-glucose-6P as the source of carbohydrate. Instead, all of the five strains used D-fructose-6P (PM1, well E04), which is also one of the intermediates of glycolysis. This implies that glucose does not serve as the preferred carbohydrate source for all the *H. pylori* strains. Nevertheless, the lack of the enzymes fructose-6-phosphokinase (which phosphorylates β-D-fructose-6P) and pyruvate kinase (which converts phosphoenolpyruvate to pyruvate) diverts D-fructose-6P away from the glycolytic pathway. As supported by earlier studies [19,20], *H. pylori* consists of two complete pathways for carbohydrate metabolism: the Entner–Doudoroff and the nonoxidative pentose phosphate pathways. Although not utilized by all the strains, D-fructose-6P can be converted to D-glucose-6P by glucose-6-phosphate isomerase, which enters the Entner–Doudoroff pathway to produce pyruvate. The utilization of D-glucuronic acid by all the strains implies that the bacteria could convert this compound into 6-phospho-D-gluconate in the Entner–Doudoroff pathway. However, the corresponding enzymes are yet to be identified as no orthologues were found in this study. Furthermore, the lack of phosphogluconate dehydrogenase in the oxidative pentose phosphate pathway means that the bacterium is not able to convert 6-phospho-D-gluconate into D-ribulose-5P, shunting the carbon into the Entner–Doudoroff pathway. Metabolism of other pentose compounds such as L-arabinose (PM1, well A02), D-xylose (PM1, well B08), D-ribose (PM1, well C04), L-lyxose (PM1, well H06), and D-arabinose (PM2, well B05) by all the strains also implies that the *H. pylori* uses the pentose phosphate pathway. Expectedly, deoxyribose/2-deoxy-D-ribose (PM2, well B09), which serves as an important precursor in DNA biosynthesis, was also utilized by all the strains. Alternative sugar sources for all the five strains of *H. pylori* include D-psicose (PM1, well H05). This hexose can be converted to fructose by D-psicose 3-epimerase, which orthologue was identified in the *H. pylori* genome.

The TCA cycle in *H. pylori* has been reported to appear as a noncyclic pathway because of the absence of the enzymes succinyl-CoA synthetase and malate dehydrogenase [21]. As shown in the KEGG pathway prediction in Fig. 4, the dicarboxylic acid arm proceeds reductively from malate through fumarate to succinate and the tricarboxylic acid arm operates oxidatively from oxaloacetate through citrate, cis-aconitrate, isocitrate, oxalosuccinate, α-ketoglutarate to succinyl-CoA. Instead of having α-ketoglutarate dehydrogenase, all the *H. pylori* strains tested in this study encode for α-ketoglutarate ferredoxin oxidoreductase to catalyze the conversion of α-ketoglutarate to succinyl-CoA. The compounds of the TCA cycle that were tested in the PM assays include malate (PM1, well G11), fumarate (PM1, well F05), succinate (PM1, well A05), citrate (PM1, well F02), and α-ketoglutarate (PM1, well D06). Citrate was only utilized by the strains J99 and UM276, whereas α-ketoglutarate was only utilized by the strains J99 and UM066. On the contrary, malate, fumarate, and succinate were metabolized by all the strains, suggesting that the dicarboxylic acid arm is the preferred pathway of the TCA cycle by local strains of *H. pylori*. Furthermore, the absence of oxidative reactions in pentose phosphate pathway and TCA cycle explains the microaerophilic nature of *H. pylori*.

Lack of metabolic activity in the well-containing β-cyclodextrin (PM2, well A04) gives an interesting insight. β-cyclodextrin has been added into liquid medium for the cultivation of *H. pylori*. Studies [22–24] showed the β-cyclodextrin-supplemented culture broth enhanced *H. pylori* growth without interfering with the expression of antigens or toxins in *H. pylori*. Nevertheless, the study by Walsh et al. [25] showed contradictory results whereby there was inhibition of growth of some *H. pylori* strains in the β-cyclodextrin-supplemented media. The results of the present investigation confirm that the β-cyclodextrin has no nutritional value to the *H. pylori* metabolism. Instead, this cyclic oligosaccharide removes toxic fatty acids from the media [26]. This indicates that BHI supplemented with yeast extract used in this study has sufficient nutrients to support *H. pylori* growth.

Iwatani et al. [27] identified the genes contributing to the lactate utilization and demonstrated that *H. pylori* is able to utilize both D- and L-lactate. It was reported that the gene *hp0137* in strain 26695 involved in the utilization of lactate contribute to stomach colonization by *H. pylori* [28]. All the strains tested in the present study carry the orthologues of the genes that encodes for lactate dehydrogenase (*hp1222* in strain 26695) and the corresponding genes, including *hp0137*. However, only certain strains have the ability to catabolize lactate. As the strains UM037 and UM066 did not respire with K-lactate (PM1, well B09), this suggests that lactate metabolism is not the consensus virulence factor in *H. pylori* infection.

Amino acid Metabolism

Utilization of amino acid as carbon and nitrogen sources in *H. pylori* has been described. In the earlier

reports [29–31], arginine, isoleucine, leucine, methionine, phenylalanine, and valine were mainly consumed during the growth of *H. pylori* of strains of Australian and European isolates. However, the diversity in the requirements for these amino acids is demonstrated in the present study.

In addition to being involved in carbon metabolism, three of the amino acids that serve as core carbon nutrients to *H. pylori* also serve as important nitrogen sources to the bacteria; these are L-aspartic acid (PM1, well A07; PM3, well A10), D-alanine (PM1, well A09; PM3, well C03), and L-asparagine (PM1, well D01; PM3, well A09). The results showed that carbohydrates could be removed from the media in which amino acids constituted basic nutrients. In addition to succinate and malate, aspartic acid can also be used to generate fumarate in the TCA cycle while the aspartic acid can be formed from asparagine. The PM results are in agreement with the KEGG predictions that all the strains metabolized aspartic acid and asparagine as carbon sources.

Alanine and proline have been reported as both carbon and nitrogen energy sources for the *H. pylori* strains [32]. Although the metabolism of alanine has been proven in the present study, proline metabolism showed contrasting results. Proline uptake and respiration in the infection and redox homeostasis of *H. pylori* have been characterized in previous studies [33–35]. However, L-proline (PM1, well A08; PM3, well B09) was not involved in the respiration of all *H. pylori* strains in the present study. Although *putP*, the gene responsible for proline uptake, is present in all the strains, only J99 metabolized L-proline both as carbon and nitrogen sources. UM037 did not utilize L-proline, but it serves as a carbon nutrient for UM032, UM066, and UM276.

The incomplete glycolytic pathway is also attributed by the absence of pyruvate kinase that phosphorylates phosphoenolpyruvate to pyruvate. The ability of utilizing serine by all the strains indicates that this step can be by passed through the formation of pyruvate in the carbohydrate metabolism. The KEGG pathway predicted that serine can be formed from glycerate-3P through 3P-hydroxypyruvate and phosphoserine. The catabolism of serine to produce pyruvate has been shown in an earlier study [36]. D-alanine was also used by all the strains as carbon source. Although it can be used to synthesize pyruvate, orthologues of D-alanine aminotransferase were not identified in *H. pylori*. Nonetheless, D-alanine is also required as one of the precursors in peptidoglycan biosynthesis (Fig. S3). The present results support a study by Nagata et al. that revealed the production of pyruvate from alanine and serine [37]. However, the pyruvate was produced from L-serine (PM1, well G03; PM3, well B10), instead of the D-serine (PM1, well B01) that was utilized by all the strains in the present study. Furthermore, the same study by Nagata et al. [37] also indicated that the production of ammonia from D- and L-alanine, and L-serine, which may contribute to protecting *H. pylori* from their acidic environment.

Helicobacter pylori has urease, which allows them to hydrolyze urea into ammonia and carbon dioxide. The nitrogen molecules from urea were shown to be incorporated into glutamate and glutamine in this organism by glutamate dehydrogenase and glutamine synthetase, respectively [38,39]. The activities of the enzymes in the tested strains are also predicted by KEGG (Fig. 4). Contrary to the accepted view that *H. pylori* metabolizes urea, the well A02 (ammonia) and A05 (urea) in PM3 surprisingly showed zero activities by all the tested strains. In other words, urea and ammonia were not utilized by these strains during their respiration. The glutamate dehydrogenase and glutamine synthetase, which serve as ammonium assimilation enzymes in *H. pylori*, were shown to enhance the ability of *H. pylori* to survive in an acidic environment [39]. In addition, these enzymes have been studied for their roles in host cell cytotoxicity [40,41] and in suppression of the host immune response [42]. The medium used in this PM analysis contains minimal nutrient, whereas the organism's niche in nature is the human gastric, which could be abundant in nutrients. Thus, the absence of the dye reduction signals could be explained by the absence of inducer to trigger the utilization of these nitrogen compounds. For example, nickel as cofactor for urease has been shown to increase the expression of urease and hence enhance the *H. pylori* colonization in stomach [43,44].

Ability of *H. pylori* Survival with Osmolytes

Although there is limited knowledge on the response of *H. pylori* to osmotic shock, Spohn and Scarlato [45] described the role of the HspR regulatory protein in mediating the transcriptional response to changes in temperature, salt, and/or osmotic stress. Epidemiological studies associated high-salt diets with *H. pylori* infection, as dietary sodium chloride intake emerged as a key player in enhancing the likelihood of severe disease outcomes such as gastric cancer [46]. In the current observation, PM analysis showed that *H. pylori* had positive respiration at up to 10% NaCl. Previous studies had demonstrated that at even higher salt concentrations of 30% resulted in increased expression of *H. pylori* virulence factors, including CagA [47,48]. Higher

  22: e12321, DOI: 10.1111/hel.12321

salt tolerance by the strain UM032 implies that different *H. pylori* strains evolved to withstand different NaCl pressures that could arise from specific host dietary habits. In addition, *H. pylori* could survive in the presence of other ions or osmolytes such as sodium lactate, sodium phosphate, sodium benzoate, ammonium sulfate, sodium nitrate, and sodium nitrite. These compounds are commonly present in food as additives or preservatives, suggesting that the bacteria might grow in the broad range of additives or preservatives used in food industry.

Future Works

Helicobacter pylori has implications in diverse clinical and epidemiologic scenarios. Our study has provided substantial grist for further experimental studies of *H. pylori* pathogenesis. Potential new substrates for growth media were also revealed through this study. However, more experiments are needed to fully understand the carbohydrate and amino acid catabolism in this bacterium, and these investigations should be guided by genomic data. Future work could focus on understanding the molecular basis of metabolic pathways in greater detail. This would improve understanding of the mechanisms in which *H. pylori* genes undergo changes leading to heterogeneity as the organism strives to survive in its seemingly hostile gastric niche.

Acknowledgements and Disclosures

We would like to thank Dr Barry Bochner from Biolog Inc. and Li Fen Chai from Focus Biotech Sdn. Bhd. for scientific advice and technical assistance. We also thank Dr Lay Ching Chai from Institute of Biological Sciences, University of Malaya, and Dr Markus Göker from Department of Microorganisms, DSMZ, for their guidance on PM data analysis. This work was supported by University of Malaya-Ministry of Education (UM-MoE) High Impact Research (HIR) Grant UM.C/625/1/HIR/MoE/CHAN/13/3 (Account No. H-50001-A000030). **Competing interests**: the authors declare no conflict of interest.

References

1 Mobley HL, Island MD, Hausinger RP. Molecular biology of microbial ureases. *Microbiol Rev* 1995;59:451–80.
2 Go M, Graham D. How does *Helicobacter pylori* cause duodenal ulcer disease: the bug, the host, or both? *J Gastroenterol Hepatol* 1994;9:S8–10.
3 Blaser MJ. Not all *Helicobacter pylori* strains are created equal: should all be eliminated?. *Lancet* 1997;349:1020–2.
4 Price ND, Papin JA, Palsson BØ. Determination of redundancy and systems properties of the metabolic network of *Helicobacter pylori* using genome-scale extreme pathway analysis. *Genome Res* 2002;12:760–9.
5 Marais A, Mendz GL, Hazell SL, Mégraud F. Metabolism and genetics of *Helicobacter pylori*: the genome era. *Microbiol Mol Biol Rev* 1999;63:642–74.
6 Bochner BR, Giovannetti L, Viti C. Important discoveries from analysing bacterial phenotypes. *Mol Microbiol* 2008;70:274–80.
7 Alm RA, Ling LL, Moir DT, et al. Genomic-sequence comparison of two unrelated isolates of the human gastric pathogen *Helicobacter pylori*. *Nature* 1999;397:176–80.
8 Bochner BR, Gadzinski P, Panomitros E. Phenotype Microarrays for high-throughput phenotypic testing and assay of gene function. *Genome Res* 2001;11:1246–55.
9 Aziz RK, Bartels D, Best AA, et al. The RAST Server: rapid annotations using subsystems technology. *BMC Genom* 2008;9:75.
10 Overbeek R, Begley T, Butler RM, et al. The subsystems approach to genome annotation and its use in the project to annotate 1000 genomes. *Nucleic Acids Res* 2005;33:5691–702.
11 Altschul SF, Gish W, Miller W, Myers EW, Lipman DJ. Basic local alignment search tool. *J Mol Biol* 1990;215:403–10.
12 Rehvathy V, Tan H, Gunaletchumy SP, et al. Multiple genome sequences of *Helicobacter pylori* strains of diverse. *Genome Announc* 2013;1:e00687–13.
13 Khosravi Y, Rehvathy V, Wee WY, et al. Comparing the genomes of *Helicobacter pylori* clinical strain UM032 and mice-adapted derivatives. *Gut Pathog* 2013;5:25.
14 Bode G, Mauch F, Ditschuneit H, Malfertheiner P. Identification of structures containing polyphosphate in *Helicobacter pylori*. *J Gen Microbiol* 1993;139:3029–33.
15 Shirai M, Kakada J, Shibata K, Morshed MG, Matsushita T, Nakazawa T. Accumulation of polyphosphate granules in *Helicobacter pylori* cells under anaerobic conditions. *J Med Microbiol* 2000;49:513–9.
16 Ayraud S, Janvier B, Labigne A, Ecobichon C, Burucoa C, Fauchère JL. Polyphosphate kinase: a new colonization factor of *Helicobacter pylori*. *FEMS Microbiol Lett* 2005;243:45–50.
17 Mendz GL, Hazell SL, Burns BP. Glucose utilization and lactate production by *Helicobacter pylori*. *J Gen Microbiol* 1993;139:3023–8.
18 Tomb JF, White O, Kerlavage AR, et al. The complete genome sequence of the gastric pathogen *Helicobacter pylori*. *Nature* 1997;388:539–47.
19 Mendz GL, Hazell SL, Burns BP. The Entner-Doudoroff pathway in *Helicobacter pylori*. *Arch Biochem Biophys* 1994;312:349–56.
20 Mendz GL, Hazell SL. Evidence for a pentose phosphate pathway in *Helicobacter pylori*. *FEMS Microbiol Lett* 1991;84:331–6.
21 Doig P, de Jonge BL, Alm RA, et al. *Helicobacter pylori* physiology predicted from genomic comparison of two strains. *Microbiol Mol Biol Rev* 1999;63:675–707.
22 Olivieri R, Bugnoli M, Armellini D, et al. Growth of *Helicobacter pylori* in media containing cyclodextrins. *J Clin Microbiol* 1993;31:160–2.
23 Morshed MG, Karita M, Konishi H, Okita K, Nakazawa T. Growth medium containing cyclodextrin and low concentration of horse serum for cultivation of *Helicobacter pylori*. *Microbiol Immunol* 1994;38:897–900.
24 Marchini A, D'Apolito M, Massari P, Atzeni M, Copass M, Olivieri R. Cyclodextrins for growth of *Helicobacter pylori* and production of vacuolating cytotoxin. *Arch Microbiol* 1995;164:290–3.
25 Walsh EJ, Moran AP. Influence of medium composition on the growth and antigen expression of *Helicobacter pylori*. *J Appl Microbiol* 1997;83:67–75.

26 Taneera J, Moran AP, Hynes SO, Nilsson HO, Al-Soud WA, Wadström T. Influence of activated charcoal, porcine gastric mucin and β-cyclodextrin on the morphology and growth of intestinal and gastric *Helicobacter* spp. *Microbiology* 2002;148:677–84.
27 Iwatani S, Nagashima H, Reddy R, Shiota S, Graham DY, Yamaoka Y. Identification of the genes that contribute to lactate utilization in *Helicobacter pylori*. *PLoS ONE* 2014;9:e103506.
28 Baldwin DN, Shepherd B, Kraemer P, Hall MK, Sycuro LK, Pinto-Santini DM, Salama NR. Identification of *Helicobacter pylori* genes that contribute to stomach colonization. *Infect Immun* 2007;75:1005–16.
29 Nedenskov P. Nutritional requirements for growth of *Helicobacter pylori*. *Appl Environ Microbiol* 1994;60:3450–3.
30 Reynolds DJ, Penn CW. Characteristics of *Helicobacter pylori* growth in a defined medium and determination of its amino acid requirements. *Microbiology* 1994;140:2649–56.
31 Mendz GL, Hazell SL. Aminoacid utilization by *Helicobacter pylori*. *Int J Biochem & Cell Biol* 1995;27:1085–93.
32 Stark RM, Suleiman MS, Hassan IJ, Greenman J, Millar MR. Amino acid utilisation and deamination of glutamine and asparagine by *Helicobacter pylori*. *J Med Microbiol* 1997;46:793–800.
33 Nakajima K, Inatsu S, Mizote T, Nagata Y, Aoyama K, Fukuda Y, Nagata K. Possible involvement of put A gene in *Helicobacter pylori* colonization in the stomach and motility. *Biomed Res* 2008;29:9–18.
34 Krishnan N, Becker DF. Oxygen reactivity of PutA from *Helicobacter* species and proline-linked oxidative stress. *J Bacteriol* 2006;188:1227–35.
35 Rivera-Ordaz A, Bracher S, Sarrach S, Li Z, Shi L, Quick M, Hilger D, Haas R, Jung H. The sodium/proline transporter PutP of *Helicobacter pylori*. *PLoS ONE* 2013;8:1–11.
36 Mendz GL, Hazell SL, Van Gorkom L. Pyruvate metabolism in *Helicobacter pylori*. *Arch Microbiol* 1994;162:187–92.
37 Nagata K, Nagata Y, Sato T, Fujino MA, Nakajima K, Tamura T. L-Serine, D- and L-proline and alanine as respiratory substrates of *Helicobacter pylori*: correlation between in vitro and in vivo amino acid levels. *Microbiology* 2003;149:2023–30.
38 Williams CL, Preston T, Hossack M, Slater C, McColl KE. *Helicobacter pylori* utilises urea for amino acid synthesis. *FEMS Immunol Med Microbiol* 1996;13:87–94.
39 Miller EF, Maier RJ. Ammonium metabolism enzymes aid *Helicobacter pylori* acid resistance. *J Bacteriol* 2014;196:3074–81.
40 Kim KM, Lee SG, Park MG, Song JY, Kang HL, Lee WK, Cho MJ, Rhee KH, Youn HS, Baik SC. γ-Glutamyltranspeptidase of *Helicobacter pylori* induces mitochondria-mediated apoptosis in AGS cells. *Biochem Biophys Res Commun* 2007;355:562–7.
41 Scotti C, Sommi P, Pasquetto MV, et al. Cell-cycle inhibition by *Helicobacter pylori* L-asparaginase. *PLoS ONE* 2010;5:e13892.
42 Schmees C, Prinz C, Treptau T, Rad R, Hengst L, Voland P, Bauer S, Brenner L, Schmid RM, Gerhard M. Inhibition of T-cell proliferation by *Helicobacter pylori* γ-glutamyl transpeptidase. *Gastroenterology* 2007;132:1820–33.
43 Van Vliet AHM, Kuipers EJ, Waidner B, Davies BJ, De Vries N, Penn CW, Vandenbroucke-Grauls CMJE, Kist M, Bereswill S, Kusters JG. Nickel-responsive induction of urease expression in *Helicobacter pylori* is mediated at the transcriptional level. *Infect Immun* 2001;69:4891–7.
44 Benoit SL, Miller EF, Maier RJ. *Helicobacter pylori* stores nickel to aid its host colonization. *Infect Immun* 2013;81:580–4.
45 Spohn G, Scarlato V. The autoregulatory HspR repressor protein governs chaperone gene transcription in *Helicobacter pylori*. *Mol Microbiol* 1999;34:663–74.
46 Tsugane S, Sasazuki S. Diet and the risk of gastric cancer: review of epidemiological evidence. *Gastric Cancer* 2007;10:75–83.
47 Gancz H, Jones KR, Merrell DS. Sodium chloride affects *Helicobacter pylori* growth and gene expression. *J Bacteriol* 2008;190:4100–5.
48 Xu Y, Jing J-J, Gong Y-H, Xu Q, Zhang W-L, Piao Y, Wang Y-L, Yuan Y. Changes in biological and virulent characteristics of *Helicobacter pylori* exposed to high salt. *Asian Pac J Cancer Prev* 2011;12:2637–41.

Supporting Information

Additional Supporting Information may be found online in the supporting information tab for this article:

Fig. S1 Kinetic curves of PM analysis for the five *H. pylori* strains. The raw data was extracted from OmniLog PM software and the curves were re-constructed using opm package in R-project.

Fig. S2 KEGG nitrogen metabolism pathway map constructed from the genome of the *H. pylori* J99.

Fig. S3 KEGG peptidoglycan biosynthesis pathway map constructed from the genome of the *H. pylori* J99.

Fig. S4 *H. pylori* are able to survive under various concentrations of (A) NaCl and (B) urea. The strain UM032 generally survived better in the presence of these osmolytes.

Fig. S5 pH profile of *H. pylori* metabolism. The dye reduction intensities were highest at the pH range 5.5–7. Although UM066 showed similar pattern, this strain has highest kinetic activity at pH 10, which is the highest tested in PM9.

Table S1 Nutrient sources utilized by strains in this study.

Appendix S1 Raw data (AUC) of PM analysis.

